

N95-70888

SHADOWGRAPHY OF TRANSCRITICAL CRYOGENIC FLUIDS

R. D. Woodward and D. G. Talley
USAF Phillips Laboratory
OLAC PL/RKFA
Edwards AFB, CA 93524

T. J. Anderson and M. Winter
United Technologies Research Center
East Hartford, CT 06108

SUMMARY/OVERVIEW:

The future of liquid-rocket propulsion depends heavily on continued development of high pressure liquid oxygen/hydrogen systems that operate near or above the propellant critical states; however, current understanding of transcritical/supercritical injection and combustion is yet lacking. The Phillips Laboratory and the United Technologies Research Center are involved in a collaborative effort to develop diagnostics for and make detailed measurements of transcritical droplet vaporization and combustion. The present shadowgraph study of transcritical cryogenic fluids is aimed at providing insight into the behavior of liquid oxygen or cryogenic simulants as they are injected into a supercritical environment of the same or other fluids. A detailed history of transcritical injection of liquid nitrogen into gaseous nitrogen at reduced pressures of 0.63 (subcritical) to 1.05 (supercritical) is provided. Also, critical point enhancement due to gas phase solubility and mixture effects is investigated by adding helium to the nitrogen system, which causes a distinct liquid phase to re-appear at supercritical nitrogen pressures. Liquid oxygen injection into supercritical argon or nitrogen, however, does not indicate an increase in the effective critical pressure of the system.

DISCUSSION:

Background and Objectives

To meet today's requirements for greater economy, efficiency, and reliability in space and launch propulsion, there exists a need within the liquid-rocket-propulsion community to better understand and predict mechanisms related to combustion performance, chamber wall and injector faceplate heat transfer, and combustion instabilities. This is particularly true in high pressure systems in which the fuel or oxidant (liquid oxygen in rocket propulsion systems) is injected at supercritical pressures but initially at a subcritical temperature. The propellant then undergoes a transition to a supercritical state as it is heated and burned in the combustion chamber—the so-called transcritical process. Compared with the subcritical case, transcritical and supercritical injection and combustion remain relatively poorly understood.

There are a number of differences from the subcritical case that need to be addressed. Gas/liquid density ratios are near unity, so the quasi-steady gas phase assumption commonly employed in subcritical studies is no longer valid. The equilibrium "wet bulb" condition may also not exist. Thus transcritical droplet vaporization/combustion is a fully unsteady phenomenon. The computation of properties becomes significantly more complicated in that properties such as diffusion coefficients become functions of pressure as well as temperature, and the solubility of the gas phase in the liquid phase increases significantly. The latter effect can mean that the effective critical pressure of the soluble mixture can be several times the critical pressure of the pure phase. Other property anomalies can lead to singular behavior near the critical condition. For instance, the burning rate has been observed to reach a maximum near the critical pressure, and the potential to couple with combustion instabilities may be increased. The surface tension also vanishes, potentially leading to significantly different droplet deformation and breakup mechanisms. These latter mechanisms can be particularly important because they have a direct effect on mixing.

Past experimental studies of transcritical droplet processes have been mostly limited to global measurements such as the variation of droplet lifetimes and burning times as a function of pressure [1-4]. While useful, these provide an incomplete picture of the transport and breakup mechanisms that can contribute to mixing and the potential to couple with combustion instabilities. On the other hand, the theoretical understanding of transcritical droplet vaporization, combustion, and breakup has advanced significantly in recent years due to the introduction of new models [5,6]. However, these remain unverified experimentally. The objective of work ongoing at the Phillips Lab and United Technologies Research Center (UTRC) is to provide detailed measurements of transcritical droplet flow fields and temperature and composition profiles that can be used to validate these models, as well as to develop semi-empirical correlations for direct use in comprehensive engine design codes.

Detailed measurements of droplet flow fields and temperature and composition profiles are believed to be feasible through a combination of 1) precise control of the droplet generation process to achieve repeatable, mono-sized droplets, and 2) incorporation of innovative droplet diagnostic techniques that have recently been developed [7-9]. Since the primary application at the Phillips Laboratory is rocket propulsion where the transcritical fluid is typically liquid oxygen (LOX), a piezoelectric droplet generator has been developed which is capable of producing a monodisperse stream of cryogenic droplets at high pressures. In the other arena, advanced droplet diagnostics have been under development for a number of years under AFOSR and Phillips Laboratory funding by several researchers [7-9]. These have been limited almost exclusively to subcritical droplets. Application of these and other techniques is currently being evaluated in a collaborative effort with UTRC. At present, Raman imaging appears attractive at high pressures due to the increased signal from the high molecular number density, and can potentially provide both species and temperature measurements. As part of the collaborative effort, a preliminary study of Raman imaging of LOX droplets at high pressures has been performed at UTRC facilities. The shadowgraph study emphasized in this paper was conducted in support of that effort and was aimed at understanding some of the practical issues involved before extensive application of the advanced diagnostic techniques.

Cryogenic Droplet Generation

The cryogenic droplet generator is supplied with high-pressure gaseous oxygen (or nitrogen) that is condensed within an annular liquid nitrogen heat exchanger. The main droplet generator components include a 7 micron filter, a cylindrical piezo-electric crystal (piezo), and a 127 μm (.005") diameter sapphire orifice. With electrical excitation, the piezo transmits an oscillatory disturbance to the condensed oxygen. In cryogenic operation, the device has been run in an augmented Rayleigh breakup mode for creating a droplet stream. A low-speed LOX jet is established at the droplet generator exit, then the piezo excitation is adjusted to augment the natural frequencies of the jet breakup. By altering the driving frequency and the flowrate, droplet size and spacing can be controlled. Typical LOX droplet sizes are 100 to 300 microns with inter-droplet spacing of 2 to 10 diameters. The generator is installed in a high pressure vessel with optical access on four sides so that the droplet stream can be observed and various diagnostic techniques can be employed. Repeatable, mono-sized LOX droplet generation has been achieved at pressures to 1200 psig in a helium environment.

Figure 1 illustrates typical LOX droplet generation at two different helium pressure environments. Figure 1(a) shows a very steady droplet stream at a pressure of 200 psig. while Fig. 1(b) shows a less steady, vigorously vaporizing stream at 1000 psig. The vaporization produces an unsteady oxygen-rich wake around each droplet that interacts with following droplets, perturbing the droplet stream trajectory. The field of view depicted in these figures is approximately 13 mm. These images were taken with a standard video-rate television camera illuminated by a

synchronized strobe pulse. All subsequent shadowgraph images used the same synchronized strobe lighting, but were recorded with an 8-bit intensified/gated camera that was setup for oxygen Raman imaging experiments.

It was uncertain if a reasonably consistent stream of LOX droplets could be generated at high pressures (above the critical pressure for pure oxygen) in for example a helium environment or at what point any apparent transcritical behavior would be observed. (Due to enhanced solubility of the gas phase in the liquid phase at high pressures and the corresponding mixture properties, transcritical effects may not be exhibited in binary systems until a chamber pressure up to several times that of the pure phase is reached.) As seen in Fig. 1(b), a fairly coherent and repeatable stream was produceable although not a trivial feat. Several effects related to the high pressure (high density) conditions were observed, e.g., enhanced vaporization (due to enhanced heat transfer) and increased droplet drag and thus noticeable droplet displacement and asphericity. Despite the high pressure effects noted, no phenomena directly attributable as supercritical behavior were observed.

Keep in mind that the temperature in the pressure vessel was typically in the range of 250-273 K, and so was always well above the critical temperature of oxygen. (See Table 1 for critical states of the propellants and simulants of interest here.) The droplet generator cooling jacket was continuously replenished with LN₂ at approximately 1 atm, and thus the initial droplet temperatures can be assumed to be near the normal boiling point of nitrogen (77 °K).

Transcritical Behavior

To understand better what could be defined as transcritical or supercritical behavior, it was decided to investigate, in a non-rigorous, macroscopic manner, the behavior of a pure substance as it transitions to supercritical conditions. Thus, experiments were conducted with transcritical injection of liquid nitrogen (LN₂) into gaseous nitrogen.

Figure 2 depicts a series of shadowgraph images of LN₂ injected through the droplet generator into gaseous nitrogen at reduced pressures (P_r , normalized by the critical pressure of N₂) of 0.63 to 1.05. In Fig. 2(a), at the subcritical chamber pressure of 300 psig ($P_r = 0.63$) a relatively coherent droplet stream can be produced. At the comparatively high density in this pressurized nitrogen environment, the character of the droplet stream is similar to that of the higher pressure LOX into helium stream shown in Fig. 2(b). At the higher subcritical pressure of 400 psig, Fig. 2(b) indicates that the droplet stream is no longer controllable. Rayleigh breakup, enabling production of a repeatable droplet stream, occurs when capillary forces are dominant. The higher Weber number environment, resulting from the higher ambient density and reduced surface tension near the critical point, changes the breakup mode to a regime where aerodynamic forces are significant and where droplet generation is unpredictable. Also, note that sporadic large drop production is simultaneously occurring at chamber pressures above 300 psig due to the condensation of gaseous nitrogen at the top of the chamber in the vicinity of the cold droplet generator exit. These droplets fall in a region close to and sometimes interspersed with the droplets exiting the generator orifice.

At pressures only slightly greater than that of Fig. 2(b) while operating under similar conditions, all signs of liquid structures disappeared. On the other hand, it was discovered that if the droplet-producing gas supply as well as the piezo were turned off, large liquid structures could be sustained at higher pressures. It might be surmised that at pressures close to the critical point, surface tension may be so low that any liquid structures of recordable size are destroyed by even the slightest flow perturbations to the point where essentially instantaneous vaporization occurs. Thus to continue the investigation while approaching the critical pressure, the mode of operation consisted of allowing condensed nitrogen to gravity feed through the droplet generator. However, under these conditions, it became uncertain whether the liquid nitrogen structures observed were originating in the droplet generator and "oozing" through the orifice essentially free of capillary

forces, or if they were originating in the chamber as condensation from the cold walls of the droplet generator housing.

Figure 2(c), at pressure nearing critical ($P_r = 0.96$), depicts a buoyancy-driven LN₂ flow that consists more of "stringy," ligament-like structures than droplets. Apparently large deformations result from small disturbances, and with insufficient surface tension to effectively reshape the liquid globs and pinch ligaments into drops, many strange-shaped liquid structures emerge. Also note that the surfaces of these structures appear somewhat fuzzy, as one might expect as critical conditions are approached.

Even closer to critical pressure ($P_r = 0.98$), Fig. 2(d) shows the same type of globular liquid structures except of much smaller characteristic dimension and with fuzzier interfaces. The liquid near the droplet generator exit especially is beginning to look cloud-like as it nears transition through the critical point. Farther downstream much of the liquid has vaporized.

At the critical pressure ($P_r = 1$), most shadowgraph visualizations indicated the presence of no liquid structures. Generally, density gradients/fluctuations were quite evident in the images. Sporadically one or two small globs with surface features would appear. As shown in Fig. 2(e), at slightly supercritical pressure ($P_r = 1.05$), small, cloud-like plumes of transcritical liquid could be seen entering the chamber occasionally. This was true also at pressures well above critical. Note that the pressure measurements quoted here are not extremely accurate ($\pm 2\%$ of critical pressure). Also recall that injection occurs initially at temperatures well below critical so that even at supercritical pressure, liquid could and should exist prior to heating to a critical state.

With mixture property effects on criticality in mind, a quick experiment was conducted to investigate the effect of adding a small amount of helium to the LN₂/nitrogen system since it was observed that LOX droplets could survive in a supercritical helium environment of at least $P_r = 1.7$ (based on pure O₂ critical pressure). With the nitrogen system at a slightly supercritical state ($P_r = 1.05$) and thus with no well-defined liquid structures present, a small flow (fraction of a gram per minute) of helium was introduced into the bottom of the chamber. Within a minute or two and before a noticeable increase in chamber pressure, the helium diffused throughout the chamber, apparently mixed with the injected nitrogen, and caused liquid structures with distinct surfaces to re-appear. (See Fig. 3(a).) Thus, the solubility of the helium into the nitrogen resulted in mixtures that were below the critical mixing point. Helium was allowed to continue flowing into the chamber for several minutes until a chamber pressure of 600 psig ($P_r = 1.26$) was reached. Total quantity of helium added was about 1 gram (to about 35 grams of N₂). Figure 3(b) illustrates the result: a stream of fairly spherical LN₂ droplets with well-defined surfaces.

Obviously, the solubility of helium into LN₂ (or hydrogen into LOX in the real case) at high pressures affects the way vaporization and mixing occur. However, what about larger molecular weight species? To broaden the picture, a few experiments were conducted with LOX into argon and into nitrogen. Both the LOX/Ar and LOX/N₂ systems appeared to experience transcritical effects very near the critical pressure of pure oxygen, i.e., no critical point enhancement due to gas phase solubility and mixture effects was observed. Thus, is critical point enhancement dependent on the size of the gas phase molecules? (If gas phase molecules are small enough to fill gaps in the clusters of the larger liquid molecules and hence provide additional molecular forces, would this be a mechanism to keep the cluster intact beyond the pure phase critical point?) Also, what effect do combustion products have in this scenario?

REFERENCES:

1. Faeth, G.M. Dominicus, D.P. Tulpinsky, J.F., and Olson, D.R., "Supercritical Bipropellant Droplet Combustion," *Twelfth Symposium (International) on Combustion*, The Combustion Institute, pp. 9-18 (1969).
2. Sato, J., Tsue, M., and Kono, M., "Effects of Natural Convection on High Pressure Droplet Combustion," *Comb. Fl.* 82: 142-150 (1990).

kHz repetition rates respectively. The beam steering optics in the order traversed by the beam included a periscope, a 45 mirror, and a focusing lens. The periscope raised the beam to the level of the test engine. The focal length of the focusing lens used was 10 cm. Absorption was chosen as the energy deposition technique due to the optical properties of RP-1 and to the high cost of the optics (large focusing lenses) needed to create a laser spark.

The test engine used in the experiment consisted of a windowed combustor section, an injector, a torch ignitor, and a heat sink nozzle (Figure 2). The combustion chamber accommodates up to four optical windows. The windows were made of coated zinc selenide for maximum transmission at 10.6 microns. Typically, only one zinc selenide window was used and the remaining window openings were fitted with metal blanks. The zinc selenide windows maintained the integrity of the chamber although significant cracks were visible at the conclusion of testing. The injector consisted of four GOX on RP-1 impinging triplet elements. The torch ignitor fired radially into the chamber. Initially, the ignitor was placed near the injector face but was moved downstream (just before the contraction section) in an effort to achieve more steady combustion. A GN_2 purge was applied at the window surfaces in the direction of the propellant flow to provide cooling. The chamber was equipped with a static pressure transducer to measure chamber pressure and a single high frequency piezoelectric transducer for measuring any induced pressure oscillations.

The length of the engine from the injector face to the throat was 8.88" and the chamber diameter was 2.06". This length combustor would have a first longitudinal mode of 2622 Hz assuming perfect mixing and equilibrium chemistry. The combustor was operated at a mixture ratio of from 1.7 to 2.5. The nominal chamber pressure was 70 psi. Unfortunately, it was difficult to maintain a steady chamber pressure during a run with the given hardware setup and there was insufficient time to remedy the problem. Due to the limited time available for testing, it was decided to attempt to initiate oscillations with the laser despite the unsteadiness in chamber pressure. During a test, the laser pulsing was usually initiated half way through a run. The laser pulsing was initiated by sending a TTL signal to a wave generator that sent a waveform to the CO_2 laser that drove at it a 50% duty cycle at a pre-set frequency. The beam was focused at a point 2.5" downstream of the injector face and about 3/4" inside the chamber. Due to the setup of the test stand, it was not possible to move the focal point closer to the injector face.

Attempts were made to drive the engine at various frequencies (2600 Hz, 3000 Hz, 5000 Hz, 5200 Hz). The variation of energy delivered versus frequency is given below (measured just before transmission through the zinc selenide window into the combustor):

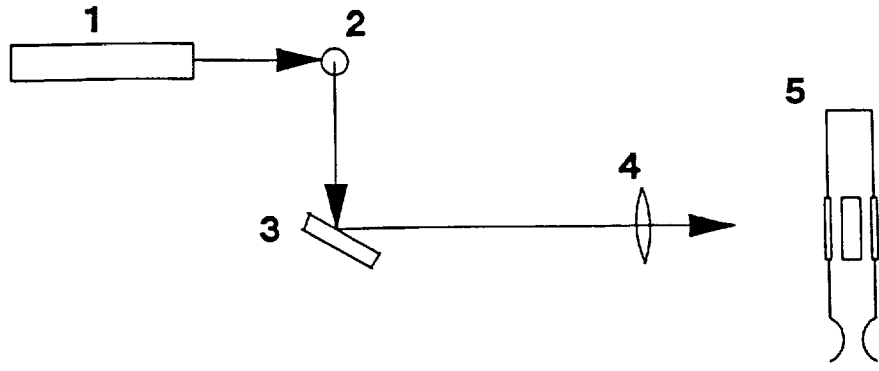
| Frequency (Hz) | Power with Wavetek (W) | Power with CA 48 (W) |
|----------------|------------------------|----------------------|
| 2000 | 60 | |
| 3000 | 65 | |
| 4000 | 66 | |
| 5000 | 67 | 85 |
| 6000 | 65 | |
| 7000 | 65 | |

The variation in power with frequency is fairly flat. The energy output of the laser peaks at 5000 Hz due to a resonance in its plasma tube. The lower power level obtained with the Wavetek signal generator at 5000 Hz is probably due to an impedance mismatch. The CA-48 was used for all testing at 5000 Hz.

No chamber pressure oscillations were recorded except when the driving frequency was 5000 Hz. When the CO₂ laser was driven at 5000 Hz, pressure oscillations at 2380 Hz were consistently recorded (Figures 3a and 3b). The amplitude of these oscillations were 2 - 2.5 psi (3% of P_c). These oscillations had a characteristic beat frequency of 125 Hz. This beating may be occurring due to the 1L oscillation (2380 Hz) going in and out of phase with the effective driving of the laser at 2500 Hz. It is interesting that no oscillations were observed when the laser was pulsed at 2600 Hz. The energy per pulse is almost double that at 5000 Hz when oscillations were observed. However, the total energy delivered at 5000 Hz is 35% higher than at 2600 Hz. Obviously, more work needs to be done to assess the feasibility of using lasers as a stability rating device. In particular, the sensitivity of the response of the combustor to the location of the focal point of the laser needs to be explored.

References

- 1) "Liquid Propellant Rocket Combustion Instability", NASA SP-194, 1972.
- 2) L. Liou, "Laser Ignition in Liquid Rocket Engines", AIAA-94-2980, 30th Joint Propulsion Conference, June 1994.



- 1. CO2 Laser
- 2. Periscope
- 3. 45 - degree mirror
- 4. Focusing lens
- 5. Test combustor

Figure 1. - Optical Setup

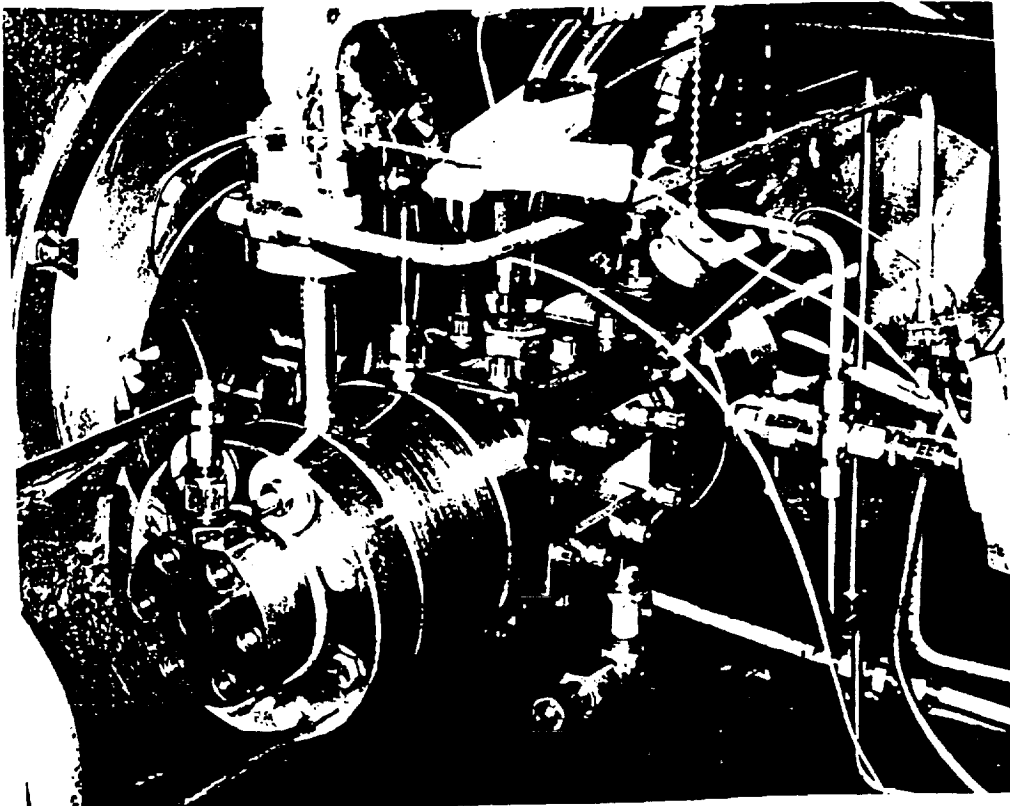


Figure 2. - Test Combustor

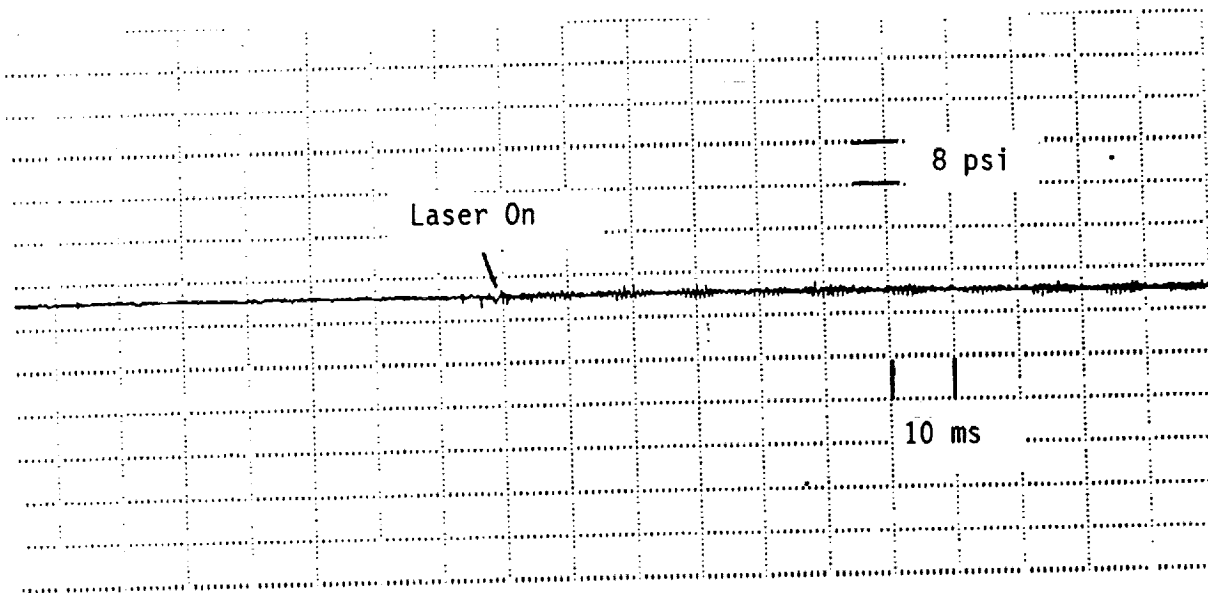


Figure 3a. - Pressure Trace

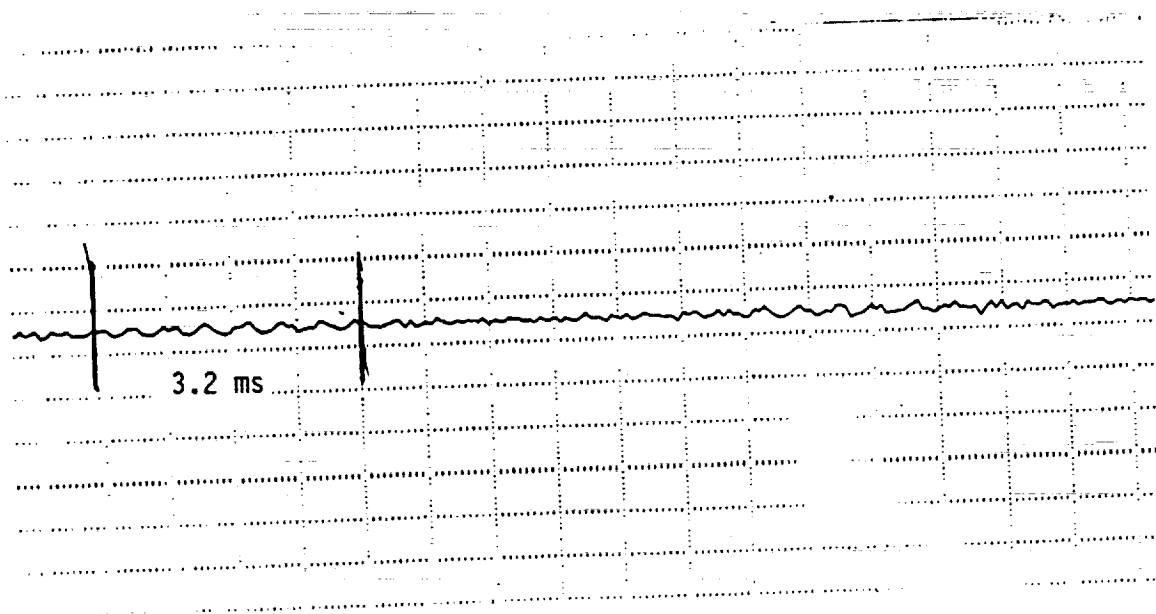


Figure 3b. - Expanded Pressure Trace

3. Natarajan, R., and Brzustowski, T.A., "Some New Observations on the Combustion of Hydrocarbon Droplets at Elevated Pressures," *Comb. Sci. and Tech.* 2: 259-269 (1970).
4. Sowles, R.E., "An Experimental Study of Carbon Dioxide Droplets Falling Through Inert High Pressure High Temperature Environments," Ph.D. Thesis, University of Wisconsin (1973).
5. Yang, V., Lin, N.N., and Shuen, J.S., "Vaporization of Liquid Oxygen (LOX) Droplets in Supercritical Hydrogen Environments," *CST* 93-01-06 (1993).
6. Delplanque, J.-P., and Sirignano, W.A., "Numerical Study of the Transient Vaporization of an Oxygen Droplet at Sub- and Supercritical Conditions," *Int. J. Heat Mass Transfer* 36: 303-314 (1993).
7. Winter, M., "Droplet Slicing Measurements of Internal Circulation," 31st AIAA Aerospace Sciences Meeting & Exhibit, Reno, NV, paper 93-0900 (1993).
8. Winter, M., and Melton, L., "Fluorescent Diagnostics and Fundamental Droplet Processes," AFOSR Contractors Meeting in Propulsion (1994).
9. Chang, R.K., "Nonlinear Optical Spectroscopy of Multicomponent Droplets," AFOSR Contractors Meeting in Propulsion (1994).

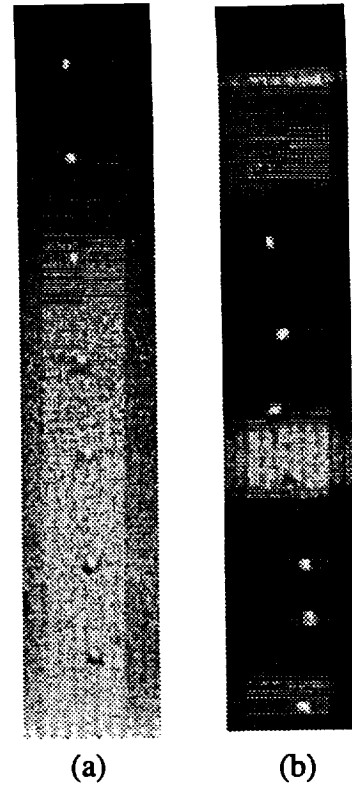
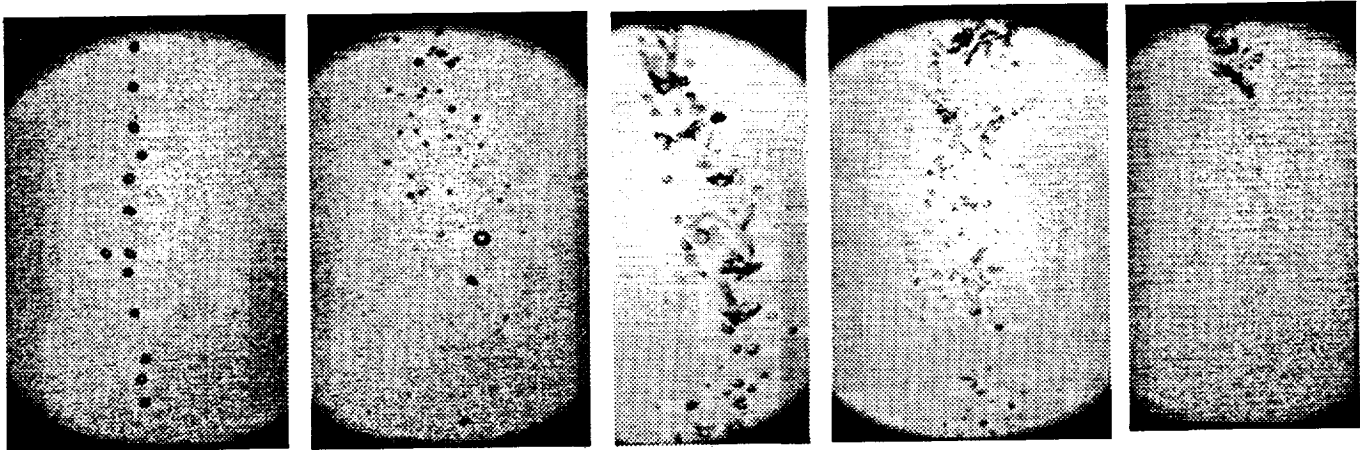
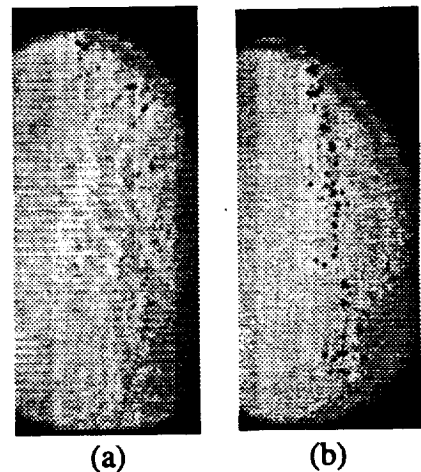


Figure 1. LOX droplet generation into helium at (a) 200 and (b) 1000 psig



P_r : (a) 0.63 (b) 0.84 (c) 0.96 (d) 0.98 (e) 1.05
Figure 2. Shadowgraphs of liquid nitrogen injection into high pressure gaseous nitrogen

Figure 3. Effect of helium introduction into the supercritical nitrogen/nitrogen system (a) immediately, 500 psig (b) after several minutes, 600 psig



| | H ₂ | He | N ₂ | O ₂ | Ar |
|---------------------------|----------------|-------|----------------|----------------|--------|
| Critical Pressure (atm) | 13 | 2.336 | 34 | 50.5 | 48.8 |
| Critical Temperature (°K) | 33.15 | 5.2 | 126.25 | 154.65 | 150.75 |
| Molecular Weight | 2.016 | 4.003 | 28.016 | 32.000 | 39.94 |